Spectrochimica Acta Part A: Molecular and Biomolecular Spectroscopy 352 (2026) 127553

Contents lists available at ScienceDirect

Spectrochimica Acta Part A:
Molecular and Biomolecular Spectroscopy

journal homepage: www.journals.elsevier.com/spectrochimica-acta-part-a-molecular-and-biomolecular-spectroscopy

Undoped zinc gallogermanate nanoparticles based persistent luminescence aptasensor for the determination of bisphenol A in aquatic products

Li-Wen Zhang [a,b], Zhu-Ying Yan [c], Xu Zhao [a,b], Li-Xia Yan [c], Li-Jian Chen [a,b,*], Xiu-Ping Yan [a,b,*]

[a] Institute of Analytical Food Safety, School of Food Science and Technology, Jiangnan University, Wuxi 214122, China
[b] Key Laboratory of Screening, Prevention, and Control of Food Safety Risks, State Administration for Market Regulation, Wuxi 214122, China
[c] Analysis and Testing Center, Jiangnan University, Wuxi 214122, China

HIGHLIGHTS

- A "turn-on" persistent luminescence aptasensor for bisphenol A detection was developed.
- The aptasensor showed high selectivity and low detection limit.
- The aptasensor was applied for interference-free determination of bisphenol A in fish samples.

GRAPHICAL ABSTRACT

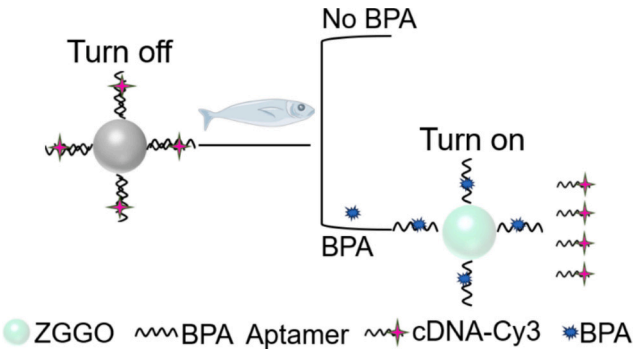

ARTICLE INFO

Keywords:
Bisphenol a
Aptasensor
Persistent luminescence
Zinc gallogermanate
Aquatic product

ABSTRACT

Bisphenol A (BPA) poses significant health risks, so its selective and sensitive determination in food is crucial. Here, we report a "turn-on" persistent luminescence aptasensor using undoped zinc gallogermanate nanoparticles (ZGGO) for selective and sensitive BPA determination in aquatic products. The sensor consists of a BPA-specific aptamer-grafted ZGGO (donor) hybridized with Cy3-labeled complementary DNA (cDNA-Cy3, acceptor). The persistent luminescence of the aptasensor is quenched via resonance energy transfer to the acceptor in the absence of BPA, and recovered in the presence of BPA due to the competitive binding of BPA with the aptamer to release cDNA-Cy3. This design effectively eliminates autofluorescence and background interference, enhancing sensitivity and selectivity. The aptasensor gives a wide linear range (1–1000 ng L^{-1}), low detection limit (0.27 ng L^{-1}), high selectivity, and good precision. Spike-recovery tests in fish samples yield the recovery of 85.2%–101.6%, proving its potential for monitoring BPA in complex food matrices.

1. Introduction

Bisphenol A (BPA) is an endocrine-disrupting chemical with a structure similar to estrogen. It can interfere with hormone metabolism, leading to endocrine disruption and health problems such as heart disease, diabetes, and obesity [1,2]. BPA, as an organic synthetic monomer

* Corresponding authors at: Institute of Analytical Food Safety, School of Food Science and Technology, Jiangnan University, Wuxi 214122, China.
E-mail addresses: chenlijian123@jiangnan.edu.cn (L.-J. Chen), xpyan@jiangnan.edu.cn (X.-P. Yan).

https://doi.org/10.1016/j.saa.2026.127553
Received 14 January 2026; Received in revised form 30 January 2026; Accepted 1 February 2026
Available online 5 February 2026

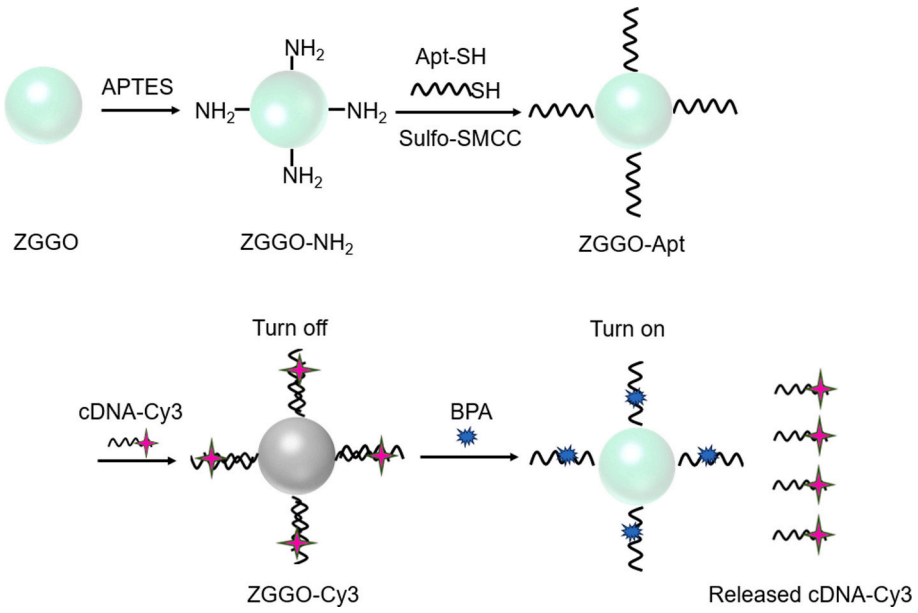

Fig. 1. Illustration for the developed ZGGO-Cy3 aptasensor for the detection of BPA.

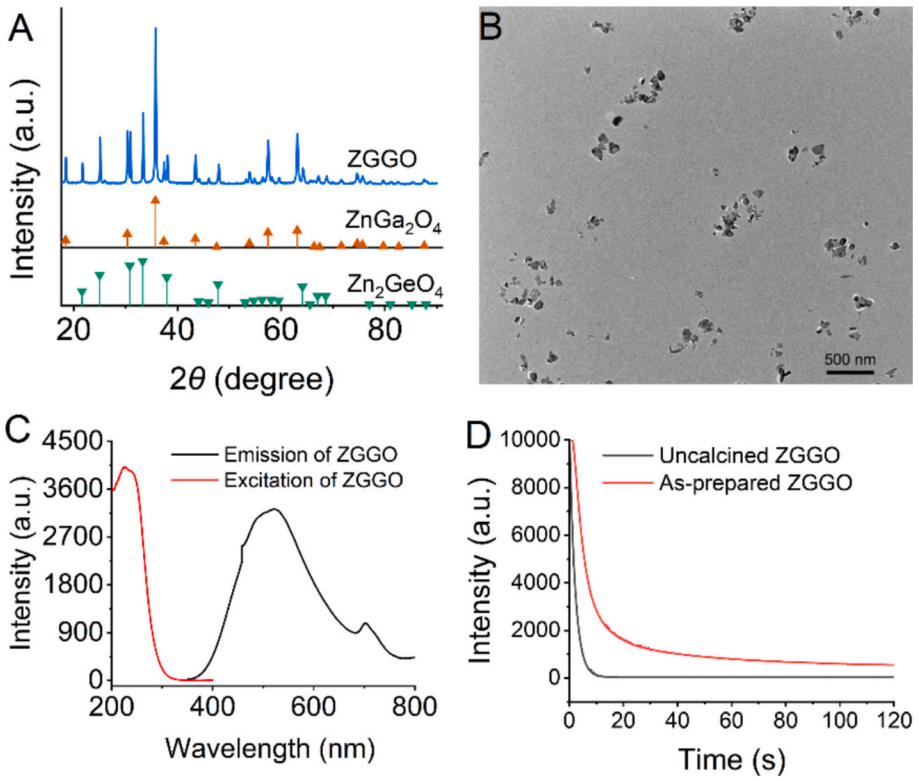

Fig. 2. (A) XRD pattern of the as-prepared ZGGO. (B) TEM image of the as-prepared ZGGO. (C) Excitation and emission spectra of the as-prepared ZGGO in aqueous solution. (D) Luminescence decay curve of the as-prepared ZGGO and the uncalcined ZGGO after 5 min irradiation with a 254 nm UV lamp.

and a widely produced plasticizer, is primarily used in the synthesis of epoxy resins and polycarbonate plastics [3–5]. Epoxy resin and polycarbonate plastics and their products are widely used in food and non-food industries due to their light weight, durability and portability [6,7]. However, BPA easily migrates into food, surface water and soil from packing materials, wastewater and landfill [8]. Following Canada's pioneering 2008 ban on BPA, countries including China and Colombia, alongside at least twelve U.S. states, have enacted their own restrictions. Furthermore, the European Food Safety Authority (EFSA) has progressively tightened its standard, reducing the Tolerable Daily Intake (TDI) twice to the current level of 0.2 ng/kg·bw/day [9]. Aquatic products, as a major component of human diet, are not only diverse in variety and delicious in taste, but also highly nutritious. They serve as an important source of high-quality protein, unsaturated fatty acids, and essential trace elements. In recent years, BPA was found in aquatic products from certain lakeside and coastal regions of China, such as Hong Kong [10], Shenzhen [11], Nanjing [12], and Wuxi [13]. Notably, the highest concentration of BPA was observed in the edible muscle

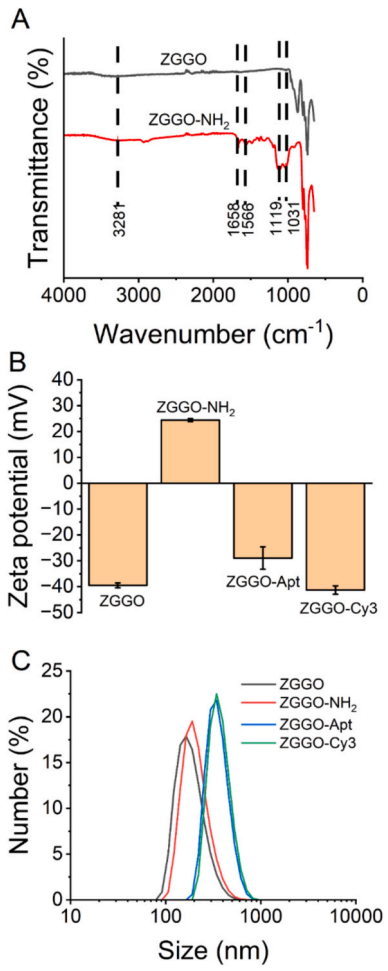

Fig. 3. (A) FT-IR spectra of ZGGO (black) and ZGGO-NH_2 (red). (B) Zeta potential of ZGGO, ZGGO-NH_2, ZGGO-Apt and ZGGO-Cy3. (C) Hydrodynamic size distribution of ZGGO, ZGGO-NH_2, ZGGO-Apt and ZGGO-Cy3. (For interpretation of the references to colour in this figure legend, the reader is referred to the web version of this article.)

tissues compared to other parts of the organisms [12], indicating that BPA contamination in aquatic products is severe and the safety of consumption needs to be taken seriously. Therefore, it is extremely necessary to detect BPA levels in aquatic products.

Currently, the main methods for the determination of BPA include high performance liquid chromatography (HPLC), liquid chromatography-mass spectrometry (LC-MS) and gas chromatography–mass spectrometry (GC–MS). These methods have the advantages of high accuracy and simultaneous detection of multiple targets, but require expensive equipment, complex sample pretreatment, and well-trained technicians [14–16]. Optical methods, especially fluorescence sensing, are rapid and highly sensitive for the detection of BPA [17]. However, the autofluorescence background of the complex food matrix often interferes with fluorescence detection [18,19].

Persistent luminescence nanoparticles can continuously emit light even after the removal of the excitation source, thereby effectively circumventing the autofluorescence interference in food matrices and enabling high signal-to-noise ratio detection. Transition metal-doped persistent luminescence nanoparticles exhibiting near-infrared (NIR) afterglow have garnered significant recent interest for sensitive optical imaging and detection [20]. For instant, a NIR persistent luminescence sensor based on $ZnGa_2O_4$:Cr^{3+} was reported for the sensitive detection of kanamycin in milk, honey, and infant formula, with a detection limit of 0.32 ng L^{-1} [21]. Furthermore, green persistent luminescence sensors based on Zn_2GeO_4:Mn^{2+} and Zn_2GeO_4:Mn^{2+},Pr^{3+} were developed for the autofluorescence-free detection of ochratoxin A in beer and aflatoxin B_1 in grains [22]. However, Zn_2GeO_4 matrix-based nanomaterials easily degrade in acidic conditions [23], constraining their potential applications. $Zn_3Ga_2Ge_2O_{10}$ (ZGGO) matrix without any metal ion doping exhibits visible emission [24], and ZGGO nanoparticles demonstrate good stability [25]. Moreover, ZGGO possesses excellent persistent luminescence properties but, to our knowledge, has not been applied to optical detection.

Aptamer, also known as chemical antibody, offers the advantages of good specificity, easy preparation, small batch-to-batch variation in synthesis, easily chemical modification, and good stability for long-term storage [26]. For the above reasons, aptamer has been widely used as recognition units in biological sensors [27–30].

In this study, we report a "turn-on" undoped ZGGO based persistent luminescence aptasensor for specific detection of BPA in aquatic products. The persistent luminescence aptasensor was developed based on resonance energy transfer strategy. The ZGGO nanoparticles modified with a BPA aptamer (Apt) [31] served as the donor, and the Cy3 fluorescent dye modified complementary chain of the aptamer acted as the receptor. The persistent luminescence of ZGGO was quenched due to the resonance energy transfer from the donor to the acceptor. However, in the presence of BPA, cDNA-Cy3 would be displaced by BPA due to its strong competitive binding with the aptamer in ZGGO-Apt to turn on the persistent luminescence. The developed aptasensor was demonstrated to effectively eliminate the background interference of food matrixes for specific detection of BPA in real samples.

2. Experimental

2.1. Materials and reagents

The BPA aptamer (5'-SH-(CH_2)6-CCG GTG GGT GGT CAG GTG GGA TAG CGT TCC GCG TAT GGC CCA-3′) and cDNA-Cy3 (5'-Cy3-CCC ACC TGA CCA CCC ACC GG-3′) (cDNA-Cy3) were purchased from Sangon Biotech (Shanghai, China). Germanium oxide (GeO_2), 4-(*N*-maleimidomethyl) cyclohexane-1-carboxylic acid 3-sulfo-*N*-hydroxysuccinimide ester sodium salt (Sulfo-SMCC), (3-aminopropyl) triethoxysilane (APTES), zinc nitrate ($Zn(NO_3)_2$), BPA, and enrofloxacin (ENR) were purchased from Aladdin (Shanghai, China). Sodium hydroxide (NaOH), tris(hydroxymethyl)aminomethane (Tris), potassium chloride (KCl), sodium chloride (NaCl), cetyltrimethylammonium bromide (CTAB), disodium hydrogen phosphate (Na_2HPO_4), potassium dihydrogen phosphate (KH_2PO_4), hydroquinone (HQ), phenol (Ph), ammonia solution, acetonitrile, and *n*-hexane were obtained from Sinopharm Chemical Reagent Co. (Shanghai, China). 4-(2-hydroxyethyl)-1-piperazineethanesulfonic acid (HEPES) was acquired from Solarbio (Beijing, China). Estriol (E3) and tetracycline hydrochloride (TC) were purchased from Macklin (Shanghai, China). *N*,*N*-dimethylformamide (DMF), methanol, and ethanol were supplied by Titan Scientific Co., Ltd. (Shanghai, China). Gallium(III) nitrate ($Ga(NO_3)_3$) was obtained from Innochem (Beijing, China). 4,4′-biphenyldicarboxylic acid (TPA) was provided by J&K Scientific (Beijing, China). Ultrapure water was purchased from Wahaha Group Co. Ltd. (Hangzhou, China).

2.2. Synthesis of ZGGO nanoparticles

The ZGGO nanoparticles were synthesized via a CTAB-assisted hydrothermal method followed by high-temperature calcination [26,32,33]. First, the precursor solutions of 0.4 M Na_2GeO_3, 2 M Zn $(NO_3)_2$, and 2 M $Ga(NO_3)_3$ were prepared. Stoichiometric volumes of Na_2GeO_3, $Zn(NO_3)_2$, and $Ga(NO_3)_3$ solutions were mixed in a beaker, followed by the addition of ultrapure water to adjust the total volume to 11 mL. Subsequently, 16 mg of CTAB was introduced into the solution under magnetic stirring. The pH of the mixture was adjusted to approximately 8.5 using ammonia solution, and the solution was

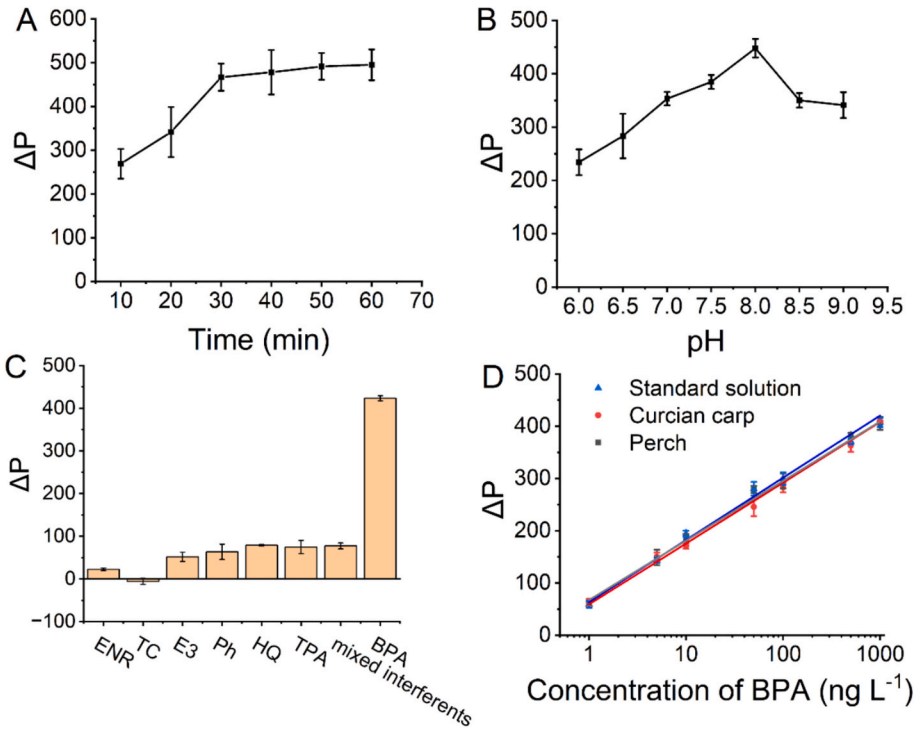

Fig. 4. (A) Effect of reaction time. (B) Effect of pH. (C) Selectivity and anti-interference ability of the developed aptasensor (Concentration: BPA, 1 μg L^{-1}; interfering substances, 10 μg L^{-1}). (D) Calibration curves for BPA standard solution and standard added fish samples.

Table 1
Matrix effects of the proposed ZGGO-Cy3 aptasensor.

Matrix	Linear range (ng L^{-1})	Regression equation	R^2	Matrix effect
Standard solution	1–1000	y = 119.0lgx + 63.4	0.9986	–
Perch	1–1000	y = 113.9lgx + 67.4	0.9957	0.9571
Crucian carp	1–1000	y = 116.3lgx + 59.1	0.9990	0.9773

Table 2
Analytical results for the proposed aptasensor for the determination of BPA in fish samples (mean ± *s*, *n* = 3).

Frozen samples	BPA concentration found (μg kg^{-1}, mean ± s, *n* = 3)		Recovery (%, mean ± s, *n* = 3)		
	This method	LC-MS	1.00 μg kg^{-1}	10.0 μg kg^{-1}	100.0 μg kg^{-1}
Perch-1	4.76 ± 0.42	4.07 ± 0.69	98.6 ± 3.2	92.7 ± 6.0	88.0 ± 2.9
Perch-2	2.29 ± 0.06	2.48 ± 0.08	92.8 ± 8.9	101.6 ± 4.3	89.6 ± 3.8
Perch-3	2.97 ± 0.22	2.57 ± 0.35	93.5 ± 3.7	91.0 ± 6.4	98.0 ± 4.6
Perch-4	2.70 ± 0.07	2.88 ± 0.04	88.6 ± 9.2	89.2 ± 3.8	85.2 ± 2.8
Crucian carp-1	1.87 ± 0.15	1.91 ± 0.29	99.3 ± 2.4	96.9 ± 6.9	93.5 ± 3.8
Crucian carp-2	2.87 ± 0.35	3.17 ± 0.32	100.0 ± 7.9	89.5 ± 8.2	90.9 ± 5.2
Crucian carp-3	2.18 ± 0.13	2.48 ± 0.30	86.9 ± 5.0	96.1 ± 11.8	93.8 ± 4.5
Crucian carp-4	2.56 ± 0.24	2.82 ± 0.08	95.9 ± 2.6	94.3 ± 1.7	94.7 ± 5.5

continuously stirred at room temperature for 1 h. The homogeneous solution was then transferred into a Teflon-lined autoclave and heated in an oven at 220 °C for 6 h. After naturally cooling to room temperature, the product was centrifuged and washed thrice with ultrapure water, and dried under vacuum at room temperature. The dried precipitate was ground into a fine powder using an agate mortar and subsequently calcined in a muffle furnace under an air atmosphere at 900 °C for 3 h, with a heating rate of 4 °C min^{-1}. Then, the product was ground, ZGGO nanoparticles were thus obtained.

2.3. Preparation of amino-functionalized ZGGO nanoparticles (ZGGO-NH_2)

Firstly, ZGGO nanoparticles were hydroxylated by NaOH etching. 50 mg of ZGGO nanoparticles were dispersed in NaOH solution (50 mL, 5 mM) in a round-bottomed flask. The mixture was ultrasonicated for 10 min and magnetically stirred at room temperature for 24 h. After the reaction, the product was separated via centrifugation, washed with ultrapure water for three times, and re-dispersed in 20 mL of DMF. Then, 200 μL of APTES was added dropwise with vigorous stirring. The reaction was carried out in an oil bath at 80 °C for 24 h. Subsequently the product was washed with DMF and anhydrous ethanol, then dried in a vacuum at room temperature overnight to obtain ZGGO-NH_2.

2.4. Preparation of ZGGO-Cy3 aptasensor

1 mg of ZGGO-NH_2 and 0.3 mg of Sulfo-SMCC were ultrasonically dispersed in 1 mL of HEPES buffer (10 mM, pH 7.2) and activated with shaking at room temperature for 2 h. The product was centrifuged and washed thrice with PBS buffer (137 mM NaCl, 2.7 mM KCl, 8.7 mM Na_2HPO_4, 1.4 mM KH_2PO_4, pH 7.4), redispersed in 1 mL of PBS, then 2 nmol of BPA aptamer was added and incubated with shaking under room temperature for 12 h. The product was centrifuged and washed with PBS buffer thrice to remove any unbound BPA aptamer to obtain the BPA aptamer-modified nanoparticles (ZGGO-Apt). Then, 1 mL of ZGGO-Apt (1 mg mL^{-1}) and 2 nmol of cDNA-Cy3 were incubated with

shaking at 37 °C for 2 h. The mixture was centrifugated to remove the unreacted cDNA-Cy3 and resulting ZGGO-Cy3 aptasensor was obtained.

2.5. Preparation of perch and crucian carp samples

Live perch (*Lateolabrax japonicus*) and crucian carp (*Carassius auratus*) were collected from local supermarkets, slaughtered, and edible fillets were sliced off immediately upon arrival at the laboratory. All fish samples were taken from the bilateral dorsal muscle. One aliquot of the edible fillets were homogenized directly using a multifunctional grinder (power: 220 V, frequency: 50 Hz) as the fresh fish samples, and another aliquot were placed in clear sealed plastic bags and frozen for two months as the frozen fish samples. The frozen fish samples were also homogenized after thawing. All the fresh and frozen samples were pretreated according to National Food Safety Standard of China (GB 5009.305–2025). Briefly, 1 g of each homogenized fish sample was placed in a 50 mL centrifuge tube, and mixed with 2 mL of ultrapure water under vortex for 30 s. Then, 5 mL of acetonitrile was added, followed by vortex mixing and ultrasonic extraction for 15 min. The mixture was then centrifuged at 1440 ×*g* for 10 min, and the supernatant was collected into a fresh 50 mL tube, then evaporated to near-dryness under nitrogen in a 40 °C water bath, redissolved with 2 mL of methanol, filtrated through 0.22 μm organic membrane, and diluted 10-fold with methanol for further analysis.

2.6. Determination of BPA

100 μL of ZGGO-Cy3 solution (1 mg mL^{-1}), 40 μL of BPA standard solution (prepared with methanol) or real sample extract solution, and 260 μL of Tris-HCl buffer (10 mM, pH 8.0) were mixed. Then, the mixture was incubated with shaking at 37 °C for 50 min. After the reaction, the persistent luminescence (PL) intensity was measured on an F-7000 fluorescence spectrophotometer (Hitachi, Japan) in phosphorescence mode with an excitation wavelength of 254 nm.

3. Results and discussion

3.1. Construction and characterization of the aptasensor for BPA detection

The construction and detection principle of the persistent luminescence aptasensor for BPA are illustrated in Fig. 1. ZGGO nanoparticles were first functionalized with APTES to introduce amino group for subsequent conjugation with the BPA aptamer. Then, sulfo-SMCC was used as the crosslinking agent to graft the BPA aptamer onto the surface of ZGGO nanoparticles to obtain ZGGO-Apt. One terminus *N*-hydroxysuccinimide ester in sulfo-SMCC formed an amide bond with the amino group in ZGGO-NH_2, while the other terminus maleimide group formed a thioether bond with the thiol group on the BPA aptamer. Further reaction of ZGGO-Apt with cDNA-Cy3 via the hybridization of the aptamer and cDNA gave the aptasensor ZGGO-Cy3.

The significant spectral overlap between the emission peak of ZGGO and the absorption peak of the fluorescent dye Cy3 allows resonance energy transfer from ZGGO to Cy3 (Fig. S1). Thus, the persistent luminescence of ZGGO-Cy3 would be quenched. The target BPA enables the persistent luminescence of ZGGO-Cy3 to turn on due to the specific binding of BPA with the aptamer to displace cDNA-Cy3 from the sensor and inhibits the resonance energy transfer. Thus, a persistent luminescence "turn on" aptasensor was constructed for detecting BPA.

As the specific recognition element for the target molecule, the grafting efficiency of the aptamer on ZGGO nanoparticle surface directly influences the recognition ability for the target molecule. Therefore, the dosage of BPA aptamer was optimized. 1 mL of ZGGO-NH_2 (1 mg mL^{-1}) was used to optimize the dosage of BPA aptamer. As the dosage of the aptamer increased, the difference of the absorbance of the aptamer at 260 nm before and after the reaction gradually increased, and reached a stable state at 2.0 nmol (Fig. S2), indicating that 2.0 nmol of the aptamer was sufficient to fully react with 1 mg of ZGGO-NH_2. For the energy receptor, cDNA-Cy3 concentration critically affects the persistent luminescence of ZGGO-Apt nanoparticles, thereby influencing detection sensitivity and dynamic range. The persistent luminescence intensity of ZGGO-Apt gradually decreased with the increase in the dosage of cDNA-Cy3, but became stable over 0.2 nmol of cDNA-Cy3 (Fig. S3). Therefore, the final dosage of cDNA-Cy3 was determined to be 0.2 nmol.

The XRD pattern of the synthesized ZGGO is highly consistent with the standard cards of $ZnGa_2O_4$ (JCPDS 71–0843) and Zn_2GeO_4 (JCPDS 11–0687) (Fig. 2A), indicating that ZGGO has high crystallinity and is a solid solution formed by cubic spinel-structured of $ZnGa_2O_4$ and Zn_2GeO_4. The synthesized ZGGO shows irregular morphology with the particle size of 72 ± 20 nm (n = 100) (Fig. 2B, Fig. S4), and uniform distribution of the elements Zn, Ga, Ge and O (Fig. S5). The actual molar ratio of each element calculated from the EDS element quantitative analysis (Fig. S6) is listed in Table S1. The synthesized ZGGO could be excited by UV light from 200 to 300 nm to give a maximum emission around 500 nm (Fig. 2C), which is assigned to the transitions of $^1T_1 \rightarrow {}^1A_1$ and $^3T_1 \rightarrow {}^1A_1$ from F^0 center [34]. Excitation by a 254 nm UV lamp gave a white-green emission (Fig. S7). Excellent persistent luminescence was observed after stopping excitation (Fig. S8). Furthermore, the persistent luminescence became brighter after calcination (Fig. 2D).

The Fourier-transform infrared (FTIR) spectrum after amino functionalization of ZGGO shows characteristic peaks for O-Si-O stretching vibrations at 1031 and 1119 cm^{-1}, along with N—H stretching vibrations at 1566, 1658, and 3281 cm^{-1} (Fig. 3A), confirming successful preparation of ZGGO-NH_2. Zeta potential measurements demonstrated a charge reversal from negative (−39.5 mV) to positive (24.4 mV) (Fig. 3B), and further verified the amino functionalization. Amino functionalization led to no significant change of the morphology and luminescence spectrum of ZGGO (Fig. S9 and Fig. S10). Subsequent conjugation of thiol-terminated phosphate-rich BPA aptamer to ZGGO-NH_2 led to a shift of the surface potential back to negative values (−28.9 mV) (Fig. 3B) and an increase of the hydrodynamic diameter from 111.3 nm to 370.6 nm (Fig. 3C). Finally, base-pair hybridization between ZGGO-Apt and cDNA-Cy3 gave ZGGO-Cy3 aptasensor in accompany with a substantial reduction in surface potential (−41.3 mV) (Fig. 3B).

3.2. Optimization of detection conditions

Important detection conditions including reaction time and solution pH were optimized to ensure sufficient binding between BPA and aptamer for maximum persistent luminescence recovery. As reaction time increased, the recovered persistent luminescence intensity (ΔP) gradually increased, and reached a plateau after 30 min (Fig. 4A). Study of the effect of pH showed that the maximum persistent luminescence recovery was observed at pH 8.0 (Fig. 4B), indicating this condition most favorably facilitates specific recognition of the aptamer and BPA.

3.3. Specificity and selectivity of the developed aptasensor

Potential interfering substances in food samples, including other contaminants and structural analogs of BPA (ENR, TC, E3, Ph, HQ, TPA) were used to test the specificity and selectivity of the developed aptasensor. The results demonstrated that only BPA produced remarked persistent luminescence, no other interfering substances caused notable luminescence change, even at 10-fold higher concentration (Fig. 4C). The mixture of six interfering substances also did not cause a significant change in luminescence intensity. These results show the excellent specificity and selectivity of the developed aptasensor for the detection of BPA.

3.4. Figures of merit for the developed ZGGO-Cy3 aptasensor

The analytical performance of the developed aptasensor was

evaluated under optimal conditions. A good linear relationship between the recovered persistent luminescence (ΔP) and the logarithm of BPA concentration (C_{BPA}, ng L^{-1}) was observed in the range of 1 to 1000 ng L^{-1} (R^2, 0.9986) (Fig. 4D). The precision of the developed aptasensor for eleven replicate detections of 20 ng L^{-1} BPA was 1.2% relative standard deviation (RSD). The detection limit (3 s) of the developed aptasensor was only 0.27 ng L^{-1}, which is lower than most previously reported methods for BPA detection (Table S2).

3.5. Validation and application to real samples

The developed aptasensor was applied to the determination of BPA in two kinds of commonly consumed fish species, namely perch and crucian carp. To investigate the matrix interference, calibration curves in fish matrix were established by the standard addition method, and compared with that in standard solution (Fig. 4D). Matrix effect (ME) was then calculated as the ratio of the slope of the calibration curves in standard solution to that in fish matrices. The ME values were in the range of 0.9571–0.9773 for the real samples (Table 1), suggesting no significant matrix interference for detecting BPA in fish samples. Therefore, the quantification of BPA in real fish samples can be achieved using the standard curve calibration. BPA was found only in one of the studied fresh fish samples (Crucian carp-4) with the concentration of 0.054 ± 0.004 μg kg^{-1}. However, it was found in all of the frozen fish samples (Table 2), likely due to the migration of BPA from the plastic bags into the fish samples during the frozen storage and thawing period. The accuracy of the developed aptasensor was demonstrated by comparing with an independent high-performance chromatography-mass spectrometry method (HPLC-MS) [35]. The concentrations of BPA in the studied fish samples determined by the developed method are in good agreement with those found by the HPLC-MS method (Table 2). In addition, the recoveries of spiked BPA in the studied fish samples at 1, 10 and 100 μg kg^{-1}ranged from 85.2%–101.6%. The above results indicate the good accuracy of the developed aptasensor for BPA determination in real samples.

4. Conclusion

We have reported a visible-light-emitting undoped $Zn_3Ga_2Ge_2O_{10}$-based persistent luminescence aptasensor for sensitive and selective detection of BPA in aquatic products. This aptasensor integrates the advantages of persistent luminescence and aptamer-specific recognition for effective elimination of autofluorescence interference and significant enhancement of detection sensitivity. It also exhibits excellent specificity and superior anti-interference capability against coexisting substances. The proposed aptasensor enables accurate determination of BPA with a wide linear range, a low detection limit and negligible matrix effect. It has been successfully applied to detect BPA in perch and crucian carp samples. The results also show that the frozen storage of fish meat in plastic bags suffered from a risk of BPA migration contamination. This work not only presents a simple and reliable method for BPA monitoring in real samples. Further study on the exploration of the developed visible-light-emitting undoped $Zn_3Ga_2Ge_2O_{10}$-based persistent luminescence aptasensor for visual detection in complex matrices is under way.

Declaration of competing interest

The authors declare that they have no known competing financial interests or personal relationships that could have appeared to influence the work reported in this paper.

Acknowledgements

This work was supported by the National Natural Science Foundation of China (No. 22206060, and 22304063), the Natural Science Foundation of Jiangsu Province, China (No. BK20231033).

Appendix A. Supplementary data

Supplementary data to this article can be found online at https://doi.org/10.1016/j.saa.2026.127553.

Data availability

Data will be made available on request.

References

[1] S.G. Liu, T. Wu, Z. Liang, Q. Zhao, W. Gao, X. Shi, A fluorescent method for bisphenol a detection based on enzymatic oxidation-mediated emission quenching of silicon nanoparticles, Spectroc. Acta Pt. A-Molec. Biomolec. Spectr. 302 (2023) 123123, https://doi.org/10.1016/j.saa.2023.123123.
[2] A. Tarafdar, R. Sirohi, P.A. Balakumaran, R. Reshmy, A. Madhavan, R. Sindhu, P. Binod, Y. Kumar, D. Kumar, S.J. Sim, The hazardous threat of bisphenol a: toxicity, detection and remediation, J. Hazard. Mater. 423 (2022) 127097, https://doi.org/10.1016/j.jhazmat.2021.127097.
[3] K. Dogra, D. Lalwani, S. Dogra, D.P. Panday, N.P. Raval, M. Trivedi, A. Mora, M.S. G. Hernandez, S.A. Snyder, J. Mahlknecht, M. Kumar, Indian and global scenarios of bisphenol a distribution and its new analogues: prevalence & probability exceedance, J. Hazard. Mater. 477 (2024) 135128, https://doi.org/10.1016/j.jhazmat.2024.135128.
[4] M.-K. Li, L.-Y. Hu, C.-G. Niu, D.-W. Huang, G.-M. Zeng, A magnetic separation fluorescent aptasensor for highly sensitive detection of bisphenol a, Sens. Actuator B-Chem. 266 (2018) 805–811, https://doi.org/10.1016/j.snb.2018.03.163.
[5] G.K. Soni, R.K. Sharma, One-pot rapid and ultrasensitive sensing strategy for endocrine disruptor bisphenol a using cationic AuNPs and aptamer, Sens. Actuator B-Chem. 390 (2023) 133968, https://doi.org/10.1016/j.snb.2023.133968.
[6] E. Baralla, V. Pasciu, M.V. Varoni, M. Nieddu, R. Demuro, M.P. Demontis, Bisphenols' occurrence in bivalves as sentinel of environmental contamination, Sci. Total Environ. 785 (2021) 147263, https://doi.org/10.1016/j.scitotenv.2021.147263.
[7] F. Vilarinho, R. Sendón, A. van der Kellen, M.F. Vaz, A.S. Silva, Bisphenol a in food as a result of its migration from food packaging, Trends Food Sci. Tech. 91 (2019) 33–65, https://doi.org/10.1016/j.tifs.2019.06.012.
[8] L. Liu, Q. Zhao, A simple fluorescence anisotropy assay for detection of bisphenol a using fluorescently labeled aptamer, J. Environ. Sci. 97 (2020) 19–24, https://doi.org/10.1016/j.jes.2020.04.016.
[9] C.C. Willhite, G.P. Daston, Bisphenol exposure, hazard and regulation, Toxicology 425 (2019) 152243, https://doi.org/10.1016/j.tox.2019.152243.
[10] Y.M. Wong, R. Li, C.K.F. Lee, H.T. Wan, C.K.C. Wong, The measurement of bisphenol a and its analogues, perfluorinated compounds in twenty species of freshwater and marine fishes, a time-trend comparison and human health based assessment, Mar. Pollut. Bull. 124 (2017) 743–752, https://doi.org/10.1016/j.marpolbul.2017.05.046.
[11] Y. Chen, X. Chen, W. Lin, J. Chen, Y. Zhu, Z. Guo, Bisphenols in aquatic products from South China: implications for human exposure, Toxics 12 (2024) 154, https://doi.org/10.3390/toxics12020154.
[12] J. Liu, J. Guo, Y. Cai, J. Ren, G. Lu, Y. Li, Y. Ji, Multimedia distribution and ecological risk of bisphenol analogues in the urban rivers and their bioaccumulation in wild fish with different dietary habits, Process Saf. Environ. Protect. 164 (2022) 309–318, https://doi.org/10.1016/j.psep.2022.06.025.
[13] Y. Bao, W. Huang, X. Hu, D. Yin, Distribution of 31 endocrine-disrupting compounds in the Taihu Lake and application of the fish plasma model, Environ. Sci. Eur. 32 (2020) 80, https://doi.org/10.1186/s12302-020-00347-0.
[14] Y. Chen, W. Nie, Z. Peng, F. Yu, J. Yang, Y. Li, Strontium oxides with enzyme-like activity: a colorimetric sensor array for highly sensitive discrimination of bisphenols, Sens. Actuator B-Chem. 364 (2022) 131869, https://doi.org/10.1016/j.snb.2022.131869.
[15] E. Sundaram, A. Manna, K. Lakshmi Servarayan, V. Sivasamy Vasantha, Colorimetric detection and bio-magnification of bisphenol a in fish organs and water sources using 3′,6′-bis(diethylamino)-2- ((3,4,5trimethyl benzylidene) amino) spiro [isoindoline −1,9′-xanthen]-3-one (BTSIXO)-Fe^{3+} ion conjugate, Food Chem. 345 (2021) 128627, https://doi.org/10.1016/j.foodchem.2020.128627.
[16] M. Jia, S. Chen, T. Shi, C. Li, Y. Wang, H. Zhang, Competitive plasmonic biomimetic enzyme-linked immunosorbent assay for sensitive detection of bisphenol a, Food Chem. 344 (2021) 128602, https://doi.org/10.1016/j.foodchem.2020.128602.
[17] G. Liu, Z. Chen, X. Jiang, D.-Q. Feng, J. Zhao, D. Fan, W. Wang, In-situ hydrothermal synthesis of molecularly imprinted polymers coated carbon dots for fluorescent detection of bisphenol a, Sens. Actuator B-Chem. 228 (2016) 302–307, https://doi.org/10.1016/j.snb.2016.01.010.
[18] Z.-Y. Yan, L. Yuan, F. Hao, X.-P. Yan, Autofluorescence-free sensing of released bisphenol a from packaging materials by a persistent luminescence aptasensor, Anal. Chem. 97 (2025) 22145–22152, https://doi.org/10.1021/acs.analchem.5c04090.

[19] Y. Li, C. Guo, J. Yuan, X. Yang, H. Ji, M. Wu, L. Wu, Y. Qin, Recent advances and prospects of persistent luminescent materials in public health applications, Chem. Eng. J. 487 (2024) 150424, https://doi.org/10.1016/j.cej.2024.150424.
[20] S. Wu, Y. Li, W. Ding, L. Xu, Y. Ma, L. Zhang, Recent advances of persistent luminescence nanoparticles in bioapplications, Nano Micro Lett. 12 (2020) 70, https://doi.org/10.1007/s40820-020-0404-8.
[21] B.-B. Wang, X. Zhao, L.-J. Chen, C. Yang, X.-P. Yan, Functionalized persistent luminescence nanoparticle-based aptasensor for autofluorescence-free determination of kanamycin in food samples, Anal. Chem. 93 (2021) 2589–2595, https://doi.org/10.1021/acs.analchem.0c04648.
[22] Y.-Y. Jiang, X. Zhao, L.-J. Chen, C. Yang, X.-B. Yin, X.-P. Yan, Persistent luminescence nanorod based luminescence resonance energy transfer aptasensor for autofluorescence-free detection of mycotoxin, Talanta 218 (2020) 121101, https://doi.org/10.1016/j.talanta.2020.121101.
[23] J. Li, X. Huang, X. Zhao, L. Chen, X. Yan, pH-responsive Torpedo-like persistent luminescence nanoparticles for autofluorescence-free biosensing and high-level information encryption, Angew. Chem. Int. Ed. 60 (2021) 2398–2405, https://doi.org/10.1002/anie.202011553.
[24] Y. Wang, L. Yu, H. Zhang, R. Zhu, Z. Meng, Competitive ELISA based on pH-responsive persistent luminescence nanoparticles for autofluorescence-free biosensor determination of ochratoxin a in cereals, Anal. Bioanal. Chem. 415 (2023) 1877–1887, https://doi.org/10.1007/s00216-023-04591-0.
[25] C. Matuszewska, T.W. Pańczuk, P.A. Tanner, K.-L. Wong, Optimization of persistent luminescence performance of zinc gallogermanates, Mater. Today Chem. 26 (2022) 101065, https://doi.org/10.1016/j.mtchem.2022.101065.
[26] L. Huang, X. Wang, S. Liu, Z.-X. Gao, Application of aptamer-based biosensor in bisphenol a detection, Chin. J. Anal. Chem. 49 (2021) 172–183, https://doi.org/10.1016/S1872-2040(20)60077-9.
[27] M.O. Caglayan, S. Şahin, Z. Üstündağ, An overview of aptamer-based sensor platforms for the detection of bisphenol-a, Crit. Rev. Anal. Chem. 54 (2024) 1320–1341, https://doi.org/10.1080/10408347.2022.2113359.
[28] M. Liu, F. Yue, Q. Kong, Z. Liu, Y. Guo, X. Sun, Aptamers against pathogenic bacteria: selection strategies and apta-assay/aptasensor application for food safety, J. Agr. Food Chem. 70 (2022) 5477–5498, https://doi.org/10.1021/acs.jafc.2c01547.
[29] P. Röthlisberger, M. Hollenstein, Aptamer chemistry, Adv. Drug Deliver. Rev. 134 (2018) 3–21, https://doi.org/10.1016/j.addr.2018.04.007.
[30] D. Verma, K.R. Ranjan, P.R. Solanki, J. Singh, M. Das Mukherjee, Review—Aptasensors: cutting-edge technologies for bisphenol a detection as an endocrine disruptor, J. Electrochem. Soc. 171 (2024) 027520, https://doi.org/10.1149/1945-7111/ad2816.
[31] M. Jia, J. Sha, Z. Li, W. Wang, H. Zhang, High affinity truncated aptamers for ultra-sensitive colorimetric detection of bisphenol a with label-free aptasensor, Food Chem. 317 (2020) 126459, https://doi.org/10.1016/j.foodchem.2020.126459.
[32] Y.-J. Li, X.-P. Yan, Synthesis of functionalized triple-doped zinc gallogermanate nanoparticles with superlong near-infrared persistent luminescence for long-term orally administrated bioimaging, Nanoscale 8 (2016) 14965–14970, https://doi.org/10.1039/C6NR04950H.
[33] J. Wang, Q. Ma, X.-X. Hu, H. Liu, W. Zheng, X. Chen, Q. Yuan, W. Tan, Autofluorescence-free targeted tumor imaging based on luminous nanoparticles with composition-dependent size and persistent luminescence, ACS Nano 11 (2017) 8010–8017, https://doi.org/10.1021/acsnano.7b02643.
[34] C. Matuszewska, T.W. Pańczuk, P.A. Tanner, K.-L. Wong, Persistent luminescence of zinc gallogermanates, J. Mater. Chem. C 9 (2021) 7200–7213, https://doi.org/10.1039/D1TC01527C.
[35] C. Yang, Y. Wang, P.-Z. Dong, Y. Li, Y.-H. Pang, Determination of bisphenols in food and its contact materials migration by magnetic solid-phase extraction coupled with LC-MS/MS, Food Biosci. 59 (2024) 104179, https://doi.org/10.1016/j.fbio.2024.104179.